Logarithmic Relaxations in Mechanical Systems

Ofer Kimchi*

A wide range of experimental systems exhibit logarithmic relaxation in response to perturbations. Here, we describe how macroscopic logarithmic relaxation can arise from an underlying ensemble of exponentially decaying variables governed by a $1/\lambda$ distribution of decay rates λ. We demonstrate that this model can predict non-monotonic relaxations exhibited by crumpled paper and elastic foams. Finally, we discuss potential further research into the physical quantities corresponding to the underlying decaying modes in these mechanical systems.

An extraordinarily diverse set of experimental systems respond to perturbation through logarithmic relaxation over a wide range of timescales. Examples of such systems include flux relaxation in superconductors [1], conductance relaxation in electron glasses [2, 3], volume relaxation in polymer glasses [4, 5], stress and volume relaxations in crumpled paper and elastic foams [6, 7], the evolution of frictional strength [8], and even rheology in various plants [9, 10]. In these examples, the response of the system to a perturbation exerted on it for a time t_w is nontrivially dependent on t_w, demonstrating that these systems maintain a "memory" of their past history.

The organization of this article is outlined here. First, we describe the typical protocol for an experiment demonstrating logarithmic relaxations. Next, we describe how the logarithmic relaxation of a macroscopic observable can result from an underlying ensemble of decoupled exponentially decaying variables which each contribute linearly to the observable. This model is contingent on the underlying ensemble having a $1/\lambda$ distribution of decay rates λ. We then specialize our discussion to the mechanical relaxations of crumpled paper and elastic foams. We demonstrate that nonmonotonic relaxations, observed experimentally in these contexts, can arise naturally from the model we had previously described. Finally, we discuss potential further research into the physical meaning of the underlying decaying modes in these mechanical systems.

The experiments we will discuss in this paper typically follow three stages [11]. In Stage I, the system is allowed to relax within an initial environment for a relatively long time. The system is thus expected to be in a metastable state when, at time $-t_w$, a perturbation to the system is applied. Stage II represents the times $-t_w < t < 0$. At time $t = 0$, the beginning of Stage III, the perturbation is removed. During Stage III, the system relaxes towards the initial metastable state. We are concerned with systems whose relaxation is logarithmic in time.

Fig. 1, reproduced from Ref. [11], displays the Stage III relaxations of four disparate systems, and demonstrates that these follow the universal relation $S(t) \sim -\log(1 + t_w/t)$, where $S(t)$ is the observed quantity undergoing relaxation. The observable in each of these four systems is: the dielectric constant in mylar, the conductances in the electron glasses indium oxide and aluminum, and the conductance in room temperature porous silicon.

The origin of the ubiquitous logarithmic decay displayed in Fig. 1 has been the subject of significant theoretical work [3, 11–19]. A promising proposal, put forth by Amir, Oreg, and Imry [3, 11, 19] is described next.

We consider a general system described by a state vector $\vec{v}$ of length $N \gg 1$. We assume that the system's state is governed by a single external parameter, E, such that for any given E_x there is a corresponding equilibrium state $\vec{v}_x^{\text{eq}}$ [20]. Near the fixed point corresponding to E_x, $\vec{v} = \vec{v}_x^{\text{eq}} + \vec{\delta v}$, and the system dynamics are given by $\frac{d\vec{\delta v}}{dt} = A^{(x)}\vec{\delta v}$. The eigenvectors of $A^{(x)}$ are represented by $\vec{x}_n$. The eigenvalues of $A^{(x)}$, λ_n^x, must be real and negative, corresponding to pure decay, and we further assume that for any x they are governed by the probability distribution

$$p(\lambda) \sim 1/\lambda \tag{1}$$

within a range $\lambda_{\min} \leq \lambda \leq \lambda_{\max}$.

For electron glasses, a detailed derivation of how such a probability distribution of eigenvalues arises given reasonable physical assumptions is provided in Ref. [3].

The response of the macroscopic observable, $S[\vec{v}(t)]$ within an experiment of the sort outlined above can now be examined analytically. In Stage I, the external parameter is set at E_a, and the system is allowed to relax towards a metastable state $\vec{v}_a^{\text{eq}}$. In stage II, E is slightly perturbed to $E_b = E_a + \delta E$. The state $\vec{v}_a^{\text{eq}}$ now represents an excited state with respect to the current value of E, and the system begins relaxing towards its new equilibrium $\vec{v}_b^{\text{eq}}$. $\vec{v}_a^{\text{eq}} - \vec{v}_b^{\text{eq}}$ can be expressed in the eigenbasis of $A^{(b)}$ as $\sum_n k_n \vec{b}_n$, yielding

$$\vec{v}(t) = \vec{v}_b^{\text{eq}} + \sum_n k_n \vec{b}_n e^{-\lambda_n^b (t+t_w)}; \quad -t_w < t < 0. \tag{2}$$

In order to describe the macroscopic relaxation towards equilibrium, we make the further crucial assumptions that each eigenmode contributes independently, linearly, and equally (at least statistically) to the macroscopic observable. For the case of electron glasses, for example, it can be shown that the eigenvectors $\vec{b}_n$ are

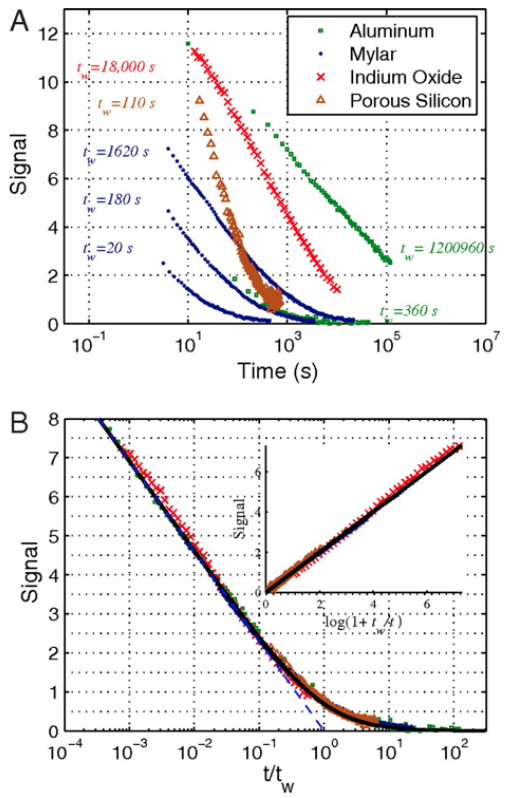

FIG. 1: (A) Logarithmic relaxations exhibited by four different systems: conductance relaxations in room temperature porous silicon and in the electron glasses indium oxide and granular aluminum, and relaxation of the dielectric constant in the plastic mylar. The signal described by the y axis thus has different units for each dataset. $t = 0$ represents the time at which the perturbation for each dataset is removed (the perturbation takes a different form for each system; see Ref. [11] for details). (B) The various curves exhibit a remarkable scaling collapse when the signal is normalized such that $S(t = t_w) = \log 2$ and t is rescaled by t_w. The inset demonstrates that the signal is described by $S(t) \sim -\log(1 + t_w/t)$ (black solid line). It is approximated by $-\log(t_w/t)$ for $t \ll t_w$ (blue dashed line) and by a power law $-t_w/t$ for $t \gg t_w$. Figure reproduced from Ref. [11].

localized, motivating the assumption that the k_n are statistically independent of n [3]. Under these assumptions, the macroscopic relaxation is given by

$$S(t) \sim \sum_n |k_n \vec{b}_n| e^{-\lambda_n^b (t+t_w)} \sim \int_{\lambda_{\min}}^{\lambda_{\max}} d\lambda \, \frac{e^{-\lambda(t+t_w)}}{\lambda}. \quad (3)$$

The RHS of Eqn. 3 can be expressed in terms of the exponential integral function, E_1. Assuming that $\lambda_{\max}^{-1} \ll t + t_w \ll \lambda_{\min}^{-1}$, Eqn. 3 can be approximated as

$$S(t) \sim -\gamma_E - \log(\lambda_{\min}(t + t_w)) \quad (4)$$

where γ_E is the Euler-Mascheroni constan. Thus as long as $\lambda_{\max} \gg \lambda_{\min}$, the macroscopic observable exhibits logarithmic decay during Stage II over a wide range of timescales.

In Stage III of the experiment, the perturbation is removed and the external parameter is set back to E_a. At time $t = 0$, the state of the system is given by $\vec{v}(0) = \vec{v}_b^{\,\mathrm{eq}} + \sum_n k_n \vec{b}_n e^{-\lambda_n^b t_w}$. In order to convert this expression to the eigenbasis of $A^{(a)}$, we use our assumption that δE is small, and thus to lowest order we can replace $\vec{b}_n$ with $\vec{a}_n$ and λ_n^b with λ_n^a. We can therefore rewrite $\vec{v}(0)$ as $\vec{v}(0) = \vec{v}_a^{\,\mathrm{eq}} + \sum_n k_n \vec{a}_n \left(e^{-\lambda_n^a t_w} - 1\right)$, arriving at

$$\vec{v}(t) = \vec{v}_a^{\,\mathrm{eq}} + \sum_n k_n \vec{a}_n \left(e^{-\lambda_n^a t_w} - 1\right) e^{-\lambda_n^a t}; \quad t > 0 \quad (5)$$

Following the same steps as in Eqn. 3, we find that the relaxation to $S(\vec{v}_a^{\,\mathrm{eq}})$ in Stage III follows the universal dynamics $S(t) \sim -\log(1 + t_w/t)$ with a nonuniversal proportionality constant. The theory thus predicts the universal dynamics of the experimental systems shown in Fig. 1.

The essence of the theory lies in the $1/\lambda$ distribution of eigenvalues of A. Processes governed by thermal activation or quantum mechanical tunneling lead naturally to this distribution, as do processes in which each relaxation rate is a product of many underlying independent variables [11]. However, for many systems undergoing logarithmic relaxation, it is still not clear what physical quantities correspond to the modes defined by λ, or even if the model is applicable. As a concrete example of such systems, we examine the mechanical relaxations of crumpled paper and elastic foams.

Experiments performed on crumpled paper [6, 7, 12] and elastic foams [6] have demonstrated that these systems relax logarithmically. However, unlike, for example, the electron glass systems analyzed in Ref. [19], the physical variables defined by λ are yet unknown for these mechanical systems. Their macroscopic nature suggests thermal activation is not at play, though their material properties preclude performing experiments in cold environments to test this claim directly. We will discuss other possibilities for the nature of the underlying ensemble distribution towards the end of this paper.

Given that the physical meaning of the underlying relaxing modes in these mechanical systems is yet undetermined, some skepticism towards the applicability of the phenomenological model discussed above is warranted. The most striking demonstration that the phenomenological model is applicable in these systems lies in recent experiments performed by Lahini *et al.* which found that under certain conditions, crumpled paper and elastic foams relax non-monotonically [6]. We will describe these experiments in detail, and then demonstrate that the non-monotonicity observed experimentally can be predicted within the context of the phenomenological model described above.

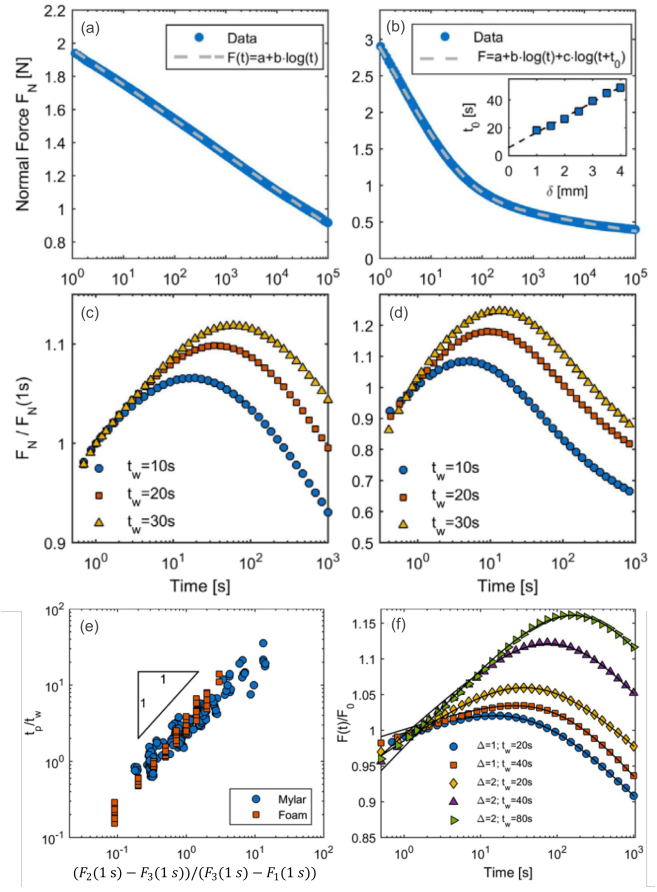

FIG. 2: Relaxation phenomena in crumpled paper and elastic foams. (a) Crumpled paper exhibits logarithmic stress relaxation. $H_a = 45$ mm; $\delta = H_a - H_b = 5$. (b) Elastic foam relaxation is well-fit to the sum of two logarithmic processes. $H_a = 18$ mm, $\delta = 4$ mm. After keeping H fixed at H_b for time t_w, H was set to $H_c = H_b + \Delta$. The resulting relaxation was non-monotonic, with nontrivial dependence on t_w. (c) results for crumpled paper with $\delta = 5$ mm, $\Delta = 2$ mm; (d) results for elastic foams with $\delta = 3$ mm, $\Delta = 1.5$ mm. (e) The time at the peak of the non-monotonic relaxation, t_p, is proportional to t_w and $\frac{F_b(1\text{ s}) - F_c(1\text{ s})}{F_c(1\text{ s}) - F_a(1\text{ s})}$ as discussed in the main text. Here, $F_i(t)$ is the normal force exerted by the material at time t after H was set to H_i. (f) This proportionality relation can be used to fit the relaxations for crumpled paper. Figure adapted from Ref. [6].

Reproducibility in experiments on crumpled paper is nontrivial as the paper is generally crumpled by hand (however, see Ref. [21]). Kramer and Lobkovsky found that in order to arrive at reproducible experiments, the paper should first be "trained" by crumpling and uncrumpling it ~ 30 times. After training, additional crumplings introduce no new ridges [22]. In their experiments, Lahini *et al.* added to the training protocol a quick compression and release of the crumpled ball before each experiment. Elastic foams require no training [6].

After training, Stage I of the experiment involved placing the paper or foam between two confining plates separated by a given distance H_a. In Stage II, corresponding to times $-t_w < t < 0$, a perturbation was applied. In the Lahini experiments, the perturbation corresponded to fixing the plate at a certain height $H_b < H_a$ and measuring the normal force exerted on the plate by the material. Previous experimenters have applied a similar protocol [12, 23] with the exception of Matan *et al.* [7] who switched the roles of stress and strain. In those experiments, a mass was placed on the top plate, and the height of the sample was measured as a function of time. Matan *et al.* demonstrated that the strain relaxed logarithmically as $a + b\log(t + t_w)$ over the several decades in time probed experimentally (from 10^{-1} to 10^6 s), and Lahini *et al.* found the same result for stress relaxation in their experiments (where times ranged from 10^0 to 10^5 s) (see Fig. 2a) [6, 7]. This behavior is predicted by Eqn. 4. Lahini *et al.* further demonstrated that after training the crumpled paper, a and b were related linearly, while no such reproducible relation was found in the absence of training (see e.g. Fig. 1b of Ref. [7]). For the case of elastic foams, the relaxation curves found by Lahini *et al.* were well-fit to the sum of two logarithmic relaxations $a + b\log(t + t_w) + c\log(t + t_w + t_0)$, where b, c, and t_0 were all linearly related to $\delta = H_a - H_b$ (Fig. 2b). As expected from the phenomenological model, logarithmic relaxations were only found for small compressions; for larger compressions, the relaxations obeyed a power law.

Lahini's experiment is notable particularly for the results in Stage III. Instead of returning the plate separation distance to H_a at time $t = 0$, Lahini set the gap to an intermediate value H_c, such that $H_b < H_c < H_a$. Remarkably, Lahini *et al.* found that the material begins relaxing *non*-monotonically: the stress first increases for a time t_p and then decreases (see Fig. 2c, d). These dynamics can be explained by the phenomenological model discussed previously, as we will now demonstrate.

Following the steps leading up to Eqn. 5, we have at $t = 0$, $\vec{v}(0) = \vec{v}_b^{\text{eq}} + \sum_n k_n \vec{b}_n e^{-\lambda_n^b t_w}$, where $\sum_n k_n \vec{b}_n = \vec{v}_a^{\text{eq}} - \vec{v}_b^{\text{eq}}$. We now seek to write this expression in terms of the eigenvectors of the metastable state corresponding to H_c, $\vec{c}_n$. We define $\sum_n k'_n \vec{c}_n = \vec{v}_c^{\text{eq}} - \vec{v}_b^{\text{eq}}$, yielding that for $t > 0$,

$$\vec{v}(t) = \vec{v}_c^{\text{eq}} + \sum_n k'_n \vec{c}_n \left(\frac{k_n}{k'_n} e^{-\lambda_n^c t_w} - 1 \right) e^{-\lambda_n^c t}; t > 0. \quad (6)$$

The non-monotonicity comes into play by recognizing that because $H_b < H_c < H_a$, $|k_n| > |k'_n|$. Therefore, the terms of the sum representing the relaxation do not all have the same sign, leading to non-monotonicity in the response of the material.

The phenomenological model is thus able to qualitatively explain the non-monotonic behavior exhibited in Lahini *et al.*'s experiments. This behavior is reminiscent of the Kovacs effect in some glassy systems which exhibit non-monotonic relaxations with the same qualitative fea-

tures [4, 5, 24–27]. While there has been significant theoretical work performed to explain the Kovacs effect [28–30] the main draw of the model we have discussed is its apparent simplicity: in this model, the observable is given by a simple linear superposition of equally contributing modes.

Furthermore the model is able to predict a scaling relation between t_p and t_w, as we will now describe. To derive this prediction, we differentiate Eqn. 6 with respect to time, setting it to zero at t_p. One of the assumptions of the model is that k_n and k'_n are statistically independent of n. Thus, when we turn the sums into integrals and assume that $\lambda_{\max}^{-1} \ll t_p \ll \lambda_{\min}^{-1}$, we get

$$t_p/t_w = k'/(k-k') \tag{7}$$

where k and k' are the averages of k_n and k'_n over n.

The values of k and k' could be determined from the $t \to \infty$ limit of Eqn. 6; however, given the logarithmic nature of the relaxation, equilibrium values cannot be probed experimentally. The key is to use the logarithmic fit parameters a and b. Letting a_i and b_i signify the fit parameters to the relaxation when $H = H_i$, $b_i - b_j$ is proportional to the difference in equilibrium stress measurements $F_i^{\text{eq}} - F_j^{\text{eq}}$. Therefore, the phenomenological model predicts that

$$\frac{t_p}{t_w} = \frac{F_b^{\text{eq}} - F_c^{\text{eq}}}{F_c^{\text{eq}} - F_a^{\text{eq}}} = \frac{F_b(t^\star) - F_c(t^\star)}{F_c(t^\star) - F_a(t^\star)} \tag{8}$$

where $t^\star$ is an arbitrary time, and we have used the proportionality of a_i and b_i to arrive at the final expression.

Eqn. 8 holds for both crumpled paper and elastic foams (the second logarithm in the force relaxation curves of foams introduces only a small correction to the above analysis). As shown in Fig. 2e, Lahini *et al.* found experimentally that the equality of Eqn. 8 should be replaced by a proportionality relation with proportionality factor $C = 2.6 \pm 0.2$. For the case of crumpled paper, Eqn. 8, along with its relation to the logarithmic fit parameters a and b, can be used to fit the non-monotonic relaxation, as shown in Fig. 2f. Whether Eqn. 8 well-describes other materials exhibiting the Kovacs effect is not yet clear, and would be an interesting experimental question.

Having demonstrated the apparent applicability of the phenomenological model to the mechanical relaxations of crumpled paper and elastic foams, we will briefly review work which could elucidate the correspondence of the modes defined by λ to physical quantities. Significant work has been performed to examine the acoustical emissions of crumpling paper [22, 31]. Each acoustical emission can be traced to a discrete physical buckling of the paper, which changes configuration as it relaxes [31]. Kramer and Lobkovsky measured the energy of each 'click' made by the paper as it relaxes, and found a power law distribution $p(E) \sim 1/E$, suggesting a connection between these emissions and the relaxation modes. Houle and Sethna repeated similar experiments, also finding that $p(E)$ obeys a power law with power $\alpha \approx -1.3$ [31]. A clue as to the origin of this power law likely lies in the crease lengths of crumpled paper, which have been shown to follow a log-normal distribution as expected of a random multiplicative process [32–34]. Far from the tails, this distribution can be approximated by a power law with $\alpha = -1$ [11]. However, it remains unclear how crease lengths are tied to relaxation rates. Some work in this direction has recently been performed by Oppenheimer and Witten who sought to probe memory effects in purely elastic materials [35] though the relationship of this work to Lahini *et al.*'s experiments is yet unclear. Another potential approach to analyze this problem would be to consider it through the lens of geometrical frustration, as in the compaction of granular media which is known to be logarithmic in time [36–39].

The relaxations of elastic foams have received much less attention compared to those of crumpling paper. In order to elucidate the underlying physical mechanism for logarithmic relaxation in this system, we turn to the field of poroelasticity. Poroelasticity describes the behavior of fluid flow within a porous, elastic material. In the elastic foams of Lahini *et al.*'s experiments, air plays the role of a fluid within the porous material. There is reason to believe simple linear poroelasticity could give rise to logarithmic relaxation: when fluid is pumped from a homogenous, isotropic, and infinite poroelastic reservoir, the pressure a distance r from the pumping site at time t after the start of pumping is given by the Theis equation [40, 41]

$$\Delta p = \frac{Q}{4\pi T} E_1\left(\frac{Sr^2}{4Tt}\right) \tag{9}$$

where Q is the rate of pumping, and S and T are poroelastic constants termed the storage coefficient and transmissivity, respectively. The exponential integral function can be approximated by a logarithm for small values of its argument, which correspond to large t. Thus, we see that pressure can change logarithmically in time within this context, even though the system is homogenous.

However, the Theis equation is not directly related to the experiments performed by Lahini *et al.*. To model those experiments in the context of linear poroelasticity, we consider a cylindrical system with a finite radius R, where inhomogeneities in the system have been coarse-grained away. The fixed strain condition is implemented by setting ϵ_{zz} to a constant (where ϵ is the strain tensor). The boundary conditions of Lahini *et al.*'s system correspond to $\sigma_{rr}(R) = p(R) = 0$, where σ is the stress tensor and p is the pore pressure. We assume that at $t = 0$ (when the boundary conditions are applied) the system is at equilibrium and has uniform pressure throughout [42].

Our preliminary results for this model are derived and discussed in the supplementary material, but suggest that the relaxation of the model is not logarithmic in time. This suggests that inhomogeneities in the elastic foam are essential to account for its logarithmic relaxation behavior.

Conclusions A wide variety of systems relax logarithmically when perturbed from a metastable state. This relaxation can be understood in many cases as resulting from an underlying ensemble of exponentially decaying variables with a $1/\lambda$ distribution of decay rates. In this model, each exponentially decaying variable contributes to the macroscopic observable linearly and equally (in the statistical sense). We demonstrated that nonmonotonic relaxations, such as have recently been observed experimentally in crumpled paper and elastic foams, can arise naturally from the model. The model further makes quantitative predictions for the behavior of t_p, the time to reach the peak of the relaxation, which are experimentally validated in the context of crumpled paper and elastic foams. However, in these systems, the model is still phenomenological. We have discussed some potential approaches to identify the physical nature of the exponentially decaying modes in these mechanical contexts, as well as preliminary original research which suggests heterogeneities in elastic foams are essential to explain their logarithmic relaxations.

ACKNOWLEDGEMENTS

I thank Ariel Amir for supervising this project and Yohai Bar-Sinai for useful discussions.

* Electronic address: okimchi@g.harvard.edu

[1] Rossel C, Maeno Y, Morgenstern I (1989) Memory effects in a superconducting Y-Ba-Cu-0 single crystal: A similarity to spin-glasses. *Physical Review Letters* 62(6):681-684.

[2] Amir A, Oreg Y, Imry Y (2010) Dynamics of electron glasses. *Annual Review of Condensed Matter Physics* 2:235-262.

[3] Amir A, Oreg Y, Imry Y (2008) Mean-field model for electron-glass dynamics. *Physical Review B* 77(16):165207

[4] Goldbach G, Rehage G (1967) Die Volumenretardation des Polystyrols nach Druck- und Temperatursprngen. *Rheologica Acta* 6(1):3053.

[5] Bernazzani P, Simon SL (2002) Volume recovery of polystyrene: evolution of the characteristic relaxation time. *Journal of Non-Crystalline Solids* 307310:470480.

[6] Lahini Y, Gottesman O, Amir A, Rubinstein SM (2017) Nonmonotonic aging and memory retention in disordered mechanical systems. *Physical Review Letters* 118(8):085501.

[7] Matan K, Williams RB, Witten TA, Nagel SR (2002) Crumpling a thin sheet. *Physical Review Letters* 88(7):076101.

[8] Ben-David O, Rubinstein SM, Fineberg J (2010) Slip-stick and the evolution of frictional strength. *Nature* 463:76-79.

[9] Thompson DS (2001) Extensiometric determination of the rheological properties of the epidermis of growing tomato fruit. *Journal of Experimental Botany* 52(359):1291-301

[10] Büntemeyer K, Lüthen H, Böttger M (1998) Auxin-induced changes in cell wall extensibility of maize roots. *Planta* 204(4):515-519.

[11] Amir A, Oreg Y, Imry Y (2011) On relaxations and aging of various glasses. *Proceedings of the National Academy of Sciences of the United States of America* 109(6):1850-5.

[12] Balankin AS, Huerta OS, Méndez FH, Ortiz JP (2011) Slow dynamics of stress and strain relaxation in randomly crumpled elasto-plastic sheets. *Physical Review E* 84(2):021118.

[13] Cugliandolo LF, Kurchan J, Ritort F (1994) Evidence of aging in spin-glass mean-field models. *Physical Review B* 49(9):6331-6334.

[14] Sibani P, Hoffmann KH (1989) Hierarchical models for aging and relaxation of spin glasses. *Physical Review Letters* 63:2853.

[15] Pleimling M, Täuber UC (2011) Relaxation and glassy dynamics in disordered type-II superconductors *Physical Review B* 84:174509.

[16] Du X, Li G, Andrei EY, Greenblatt M, Shuk P (2007) Ageing memory and glassiness of a driven vortex system *Nature Physics* 3:111-114.

[17] Shimer MT, Täuber UC, Pleimling M (2010) Nonequilibrium relaxation and scaling properties of the two-dimensional Coulomb glass in the aging regime. *Europhysics Letters* 91(6).

[18] Cugliandolo LF, Kurchan J (1993) Analytical solution of the off-equilibrium dynamics of a long-range spin-glass model. *Physical Review Letters* 71:173.

[19] Amir A, Oreg Y, Imry Y (2009) Slow Relaxations and Aging in the Electron Glass. *Physical Review Letters* 103(12):126403.

[20] In fact, $\vec{v_x}$ need not describe a true equilibrium. Any metastable state will do, provided it is far enough in phase space from other metastable states, so that when E is returned to its initial value after perturbation, the system relaxes back to its initial fixed point.

[21] Kantor Y, Kardar M, Nelson DR (1987) Tethered surfaces: Statics and dynamics. *Physical Review A* 35(7):3056-3071.

[22] Kramer EM, Lobkovsky AE (1996) Universal power law in the noise from a crumpled elastic sheet. *Physical Review E* 53(2):1465-1470.

[23] Albuquerque RF, Gomes M.A.F (2002) Stress relaxation in crumpled surfaces. *Physica A* 310(3-4):377-383.

[24] Kovacs AJ (1963) Transition vitreuse dans les polymres amorphes. Etude phnomnologique. *IFortschritte Der Hochpolymeren-Forschung. Advances in Polymer Science.* Vol 3/3. Springer, Berlin, Heidelberg.

[25] Bellon L, Ciliberto S, Laroche C (2000) Memory in the aging of a polymer glass. *Europhysics Letters* 51(5).

[26] Josserand C, Tkachenko AV, Mueth DM, Jaeger HM (2000) Memory effects in granular materials. *Physical Review Letters* 85(17-23):3632.

[27] Svoboda S, Pustková P, Máleka J (2008) Structural relaxation of polyvinyl acetate (PVAc). *Polymer* 49(1314):31763185.

[28] Bouchbinder E, Langer JS (2010) Nonequilibrium thermodynamics of the Kovacs effect. *Soft Matter* 6:3065-3073.

[29] Bertin EM, Bouchaud J-P, Drouffe J-M, Godréche C (2003) The Kovacs effect in model glasses. *Journal of Physics A* 36(43):10701-10719.
[30] Cugliandolo LF, Lozano G, Lozza H (2004) Memory effects in classical and quantum mean-field disordered models. *The European Physical Journal B* 41(1):8796.
[31] Houle PA, Sethna JP (1996) Acoustic emission from crumpling paper *Physical Review E* 54(1):278-283.
[32] Blair DL, Kudrolli A (2005) Geometry of crumpled paper. *Physical Review Letters* 94(16):166107.
[33] Balankin AS, Huerta OS, Méndez FH, Ortiz JP (2006) Intrinsically anomalous roughness of randomly crumpled thin sheets *Physical Review E* 74(6):061602.
[34] Witten T, Wood AJ (ed) (2002) Wittens lectures on crumpling. *Physica A* 313:83-109
[35] Oppenheimer N, Witten T (2015) Shapeable sheet without plastic deformation. *Physical Review E* 92:052401.
[36] Boutreux T, de Geennes PG (1997) Compaction of granular mixtures: a free volume model. *Physica A* 244(1-4):5967.
[37] Caglioti E, Loreto V, Herrmann HJ, Nicodemi M (1997) A Tetris-Like model for the compaction of dry granular media. *Physical Review Letters* 79(8):1575-1578.
[38] Nicodemi M, Coniglio A (1999) Aging in out-of-equilibrium dynamics of models for granular media. *Physical Review Letters* 82(5):916-919.
[39] Caglioti E, Coniglio A, Herrmann HJ, Loreto V, Nicodemi M (1998) Geometrical frustration: a dynamical motor for dry granular media. *Physica A* 257(1-4):419423.
[40] Theis CV (1935) The relation between the lowering of the piezometric surface and rate and duration of discharge of a well using ground water storage. *Transactions of the American Geophysical Union* 16:519524.
[41] Loáiciga HA (2010) Derivation approaches for the Theis (1935) equation *Groundwater* 48(1):1-5.
[42] We do not expect the discontinuity of p at the boundary to significantly affect our results. More precise initial conditions could be determined by considering the pressure distribution after the foam relaxes elastically, since purely elastic relaxations of the foam are expected to occur over a faster timescale than the poroelastic relaxations.

SUPPLEMENTAL INFORMATION

In the supplement, we derive the time-dependent behavior of the poroelastic system which mimics Lahini *et al.*'s experiments.

We assume that the system does not have any z dependence, except that the displacement of the solid in the z direction, u_z, is proportional to z. The symmetries of the problem dictate that the strain tensor ϵ is diagonal in polar coordinates: $\epsilon_{rr} = \partial u_r/\partial r$, $\epsilon_{\theta\theta} = u_r/r$, and ϵ_{zz} is a constant. The constant value of ϵ_{zz} models the fixed strain conditions of Lahini *et al.*'s experiments. The boundary conditions of Lahini *et al.*'s system correspond to $\sigma_{rr}(R) = p(R) = 0$, where σ is the stress tensor and p is the pore pressure. We assume that at $t = 0$ (when the boundary conditions are applied) the system is at equilibrium and has uniform pressure throughout.

The stress tensor is defined through Hooke's law, which in the context of poroelasticity becomes $\sigma_{ij} = 2G\epsilon_{ij} + \left(\frac{2G\nu}{1-2\nu}\bar{\epsilon} - \alpha p\right)\delta_{ij}$, where $\bar{\epsilon}$ is the trace of the strain tensor, and α, G and ν are poroelastic constants [1].

The boundary conditions on σ_{rr} and p can be used to determine a boundary condition on u_r:

$$\partial_r u_r(R) = \frac{-\nu}{1-\nu}\left(\frac{u_r(R)}{R} + \epsilon_{zz}\right) \tag{10}$$

This motivates us to express u_r as $u_r = u_r^h - \nu\epsilon_{zz}r$, where u_r^h satisfies

$$\partial_r u_r^h(R) = \frac{-\nu}{1-\nu}\left(\frac{u_r^h(R)}{R}\right). \tag{11}$$

Setting the divergence of σ to zero yields a proportionality relation between the spatial derivatives of p and $\bar{\epsilon}$ [1]:

$$\frac{\partial p}{\partial r} = \frac{2G(1-\nu)}{\alpha(1-2\nu)}\frac{\partial \bar{\epsilon}}{\partial r}. \tag{12}$$

This translates to

$$p = \frac{A}{r}\partial_r(ru_r) + A\epsilon_{zz} + f(t) \tag{13}$$

where $A = \frac{2G(1-\nu)}{\alpha(1-2\nu)}$ and $f(t) = -A\bar{\epsilon}(R)$

Multiplying both sides of Eqn. 13 by r and integrating dr yields

$$u_r^h(r,t) = -rg(t) + \frac{B}{r}\int_0^r dr' r' p(r',t) \tag{14}$$

where $B = 1/A$ and $g(t) = \frac{B}{2}f(t) + \left(\frac{1}{2} - \nu\right)\epsilon_{zz}$. Thus, we have expressed u_r in terms of p and $f(t)$.

$f(t)$ or $g(t)$ can further be expressed in terms of u_r^h:

$$f(t) = -A\left(\partial_r u_r(R) + \frac{u_r(R)}{R} + \epsilon_{zz}\right). \tag{15}$$

Using the boundary conditions on u_r, this simplifies to

$$f(t) = -A\left(\frac{1-2\nu}{1-\nu}\right)\left(\frac{u_r(R)}{R} + \epsilon_{zz}\right), \tag{16}$$

or

$$\begin{aligned} g(t) &= -\left(\frac{1-2\nu}{2(1-\nu)}\right)\frac{u_r(R)}{R} + \left(\frac{\nu(2\nu-1)}{2(1-\nu)}\right)\epsilon_{zz} \\ &= . - \left(\frac{1-2\nu}{2(1-\nu)}\right)\frac{u_r^h(R)}{R} \end{aligned} \tag{17}$$

While this equation could be simplified further and combined with Eqn. 14, it's not useful to do so now. Instead, we introduce the equation governing the time-dependent behavior of the system. The time-dependence of the problem is introduced via Darcy's law, which in this context takes the form [1]

$$\frac{k}{\mu}\nabla^2 p = \alpha\frac{\partial \bar{\epsilon}}{\partial t} + S_\epsilon\frac{\partial p}{\partial t} \tag{18}$$

where k, μ, and S_ϵ are poroelastic constants.

In terms of u_r, Eqn. 18 becomes

$$\frac{k}{\mu}\nabla^2 p = \alpha\left(\partial_r + 1/r\right)\partial_t u_r^h + S_\epsilon\partial_t p. \tag{19}$$

This can be written in terms of $g(t)$ (by differentiating Eqn. 14 with respect to time) as

$$\frac{k}{\mu}\nabla^2 p = C\dot{p} - 2\alpha\dot{g}(t), \tag{20}$$

where $C = B + S_\epsilon$.

Using Eqn. 17 in concert with Eqn. 14 evaluated at $r = R$, we find a relation for $g(t)$ in terms of p:

$$\dot{g}(t) = \frac{-(1-2\nu)B}{R^2}\int_0^R dr' r' \dot{p}(r'). \tag{21}$$

Plugging this into Eqn. 20, we arrive at an equation that only depends on p:

$$\frac{k}{\mu}\nabla^2 p(r,t) = C\dot{p}(r,t) + \frac{D}{R^2}\int_0^R dr' r' \dot{p}(r',t) \tag{22}$$

where $D = 2\alpha(1-2\nu)$.

This is now solvable by assuming p takes the form $p(r,t) = \sum_n \rho_n(r) T_n(t)$ (i.e. p is a linear superposition of separable solutions). T_n is easy to solve for and yields exponential decay in each mode: $T_n = c_n \exp(-nt)$. The equation for ρ is more cumbersome:

$$\frac{k}{\mu}\nabla^2\rho(r) = -nC\rho(r) - \frac{nD}{R^2}\int_0^R dr' r' \rho(r'). \tag{23}$$

We guess a solution of the form $\rho = J_0(r/a_n) - J_0(R/a_n)$ (where J is the Bessel function of the first kind) which satisfies the boundary conditions of the problem. The a_n's are found to be related to n by

$$n = \frac{k}{\mu C} a_n^{-2}. \tag{24}$$

Self-consistency of the ansatz leads to a discretization condition on n:

$$J_0\left(\frac{R}{a_n}\right) = \left(\frac{C}{D} + \frac{1}{2}\right)^{-1} \frac{a_n}{R} J_1\left(\frac{R}{a_n}\right). \tag{25}$$

and the c_n are defined by the initial conditions. In our problem, the system starts with $p = p_0$ throughout the material. Using the orthogonality of the Bessel functions, the c_n's are given by

$$c_n = \frac{p_0}{J_0\left(\frac{R}{a_n}\right)} \left(\frac{2H}{1 + H^2\left(\frac{R}{a_n}\right)^2}\right) \left(1 + \sum_m \frac{2H}{J_0\left(\frac{R}{a_m}\right)\left(1 + H^2\left(\frac{R}{a_m}\right)^2\right)}\right)^{-1} \tag{26}$$

where $H = \frac{C}{D} + \frac{1}{2}$.

All together,

$$p(r,t) = \sum_n c_n e^{-\frac{k}{\mu C}\frac{t}{a_n^2}} \left(J_0\left(\frac{r}{a_n}\right) - J_0\left(\frac{R}{a_n}\right)\right), \tag{27}$$

where the n's are discretized to be solutions of Eqn. 25, and the c_n's are given by Eqn. 26.

For large values of n, the discretization condition reduces to the zeros of J_1, and thus leads to near-uniform probability distribution $p(a_n^{-1})$. The decay rates $\lambda \sim a_n^{-2}$ are thus distributed with a $1/\sqrt{\lambda}$ probability distribution. The Ariel Oreg and Imry model therefore doesn't directly apply – the modes are not distributed with a $1/\lambda$ probability distribution. Furthermore, for large n, the c_n's are proportional to $1/J_0(R/a_n)$ where $J_1(R/a_n) = 0$. This term approximately cancels out the ρ_n term (i.e. $J_0(r/a_n) - J_0(R/a_n)$). Thus, neither of these terms affects the $1/\sqrt{\lambda}$ amplitude with which the λ modes decay.

The force this system would exert on a plate compressing it is $F(t) = \int_0^R dr\ r\sigma_{zz}(r,t)$. Given our results for $p(r,t)$, we would not expect to see logarithmic decay in $F(t)$. However, more work needs to be done to validate this intuition, by finding a closed-form solution for $F(t)$. Furthermore, more work needs to be done to approximate the natural timescale of the problem – this would involve making order-of-magnitude estimates for the values of the poroelastic constants, which we have not done here. Finally, while we have argued that pressure does not decay logarithmically in this system, this claim should be validated by numerics, which we have not performed here.

Our results should be considered extremely preliminary, but suggest that a homogenous poroelastic system with boundary conditions akin to those in Lahini *et al.*'s experiments does not undergo logarithmic relaxation. Therefore, inhomogeneities in the elastic foam are essential to account for its logarithmic behavior.

* Electronic address: okimchi@g.harvard.edu

[1] Wang HF (2000). Theory of Linear Poroelasticity with Applications to Geomechanics and Hydrogeology *Princeton University Press.*